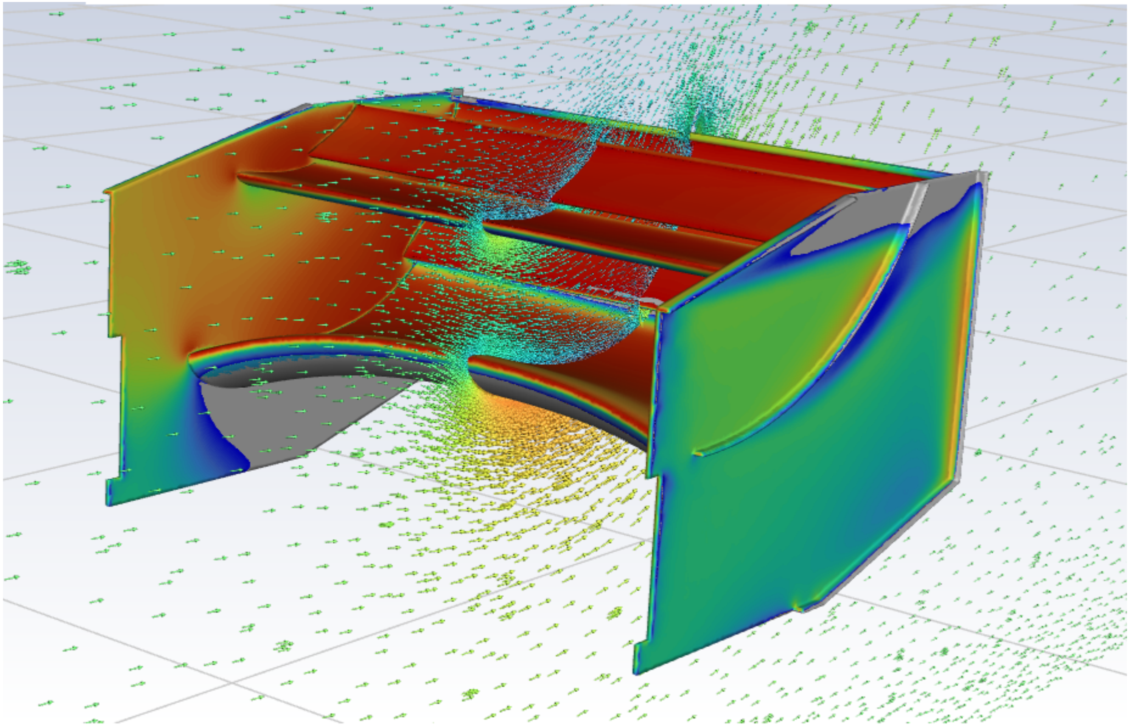

Fluid-Structure Interaction Analysis On The Rear Wing Of A Formula Student Car

Adam Kasicka

Bilal Mohammed Sajjad Siddiqui

Maulik Rakesh Rajput

DEPARTMENT OF MECHANICAL ENGINEERING

CHALMERS UNIVERSITY OF TECHNOLOGY & UNIVERSITY OF GOTHENBURG
Gothenburg, Sweden 2025
www.chalmers.se & www.gu.se

Fluid-Structure Interaction Analysis On The Rear Wing Of A Formula Student Car

ADAM KASICKA
BILAL MOHAMMED SAJJAD SIDDIQUI
MAULIK RAKESH RAJPUT
Department of Mechanical Engineering
Chalmers University of Technology and University of Gothenburg
University of Gothenburg

Abstract

This project aims to conduct a fluid structure interaction analysis on the rear wing to understand the amount of deformation in the structure due to negative lift generation. In turn, the manufacturing method is briefly discussed to evaluate how the component can be reinforced.

List of Acronyms

Below is the list of acronyms that have been used throughout this thesis, listed in alphabetical order:

AoA	Angle of Attack
CFD	Computational Fluid Dynamics
CFRP	Carbon Fiber Reinforced Polymer
CSM	Computational Structural Mechanics
FEM	Finite Element Method
FSI	Fluid Structure Interaction
GFRP	Glass Fiber Reinforced Polymer
PAN	Polyacrylo Nitrile
PVC	Polyvinyl Chloride

Contents

1
Introduction

1.1 Background

Fluid-Structure Interaction (FSI) refers to the complex relationship between fluid flow and the structural behavior of a component. It examines how fluid forces and pressure distributions influence structural properties such as deformation and stress, while also considering how structural changes impact the fluid flow. This dynamic interaction is essential for understanding various engineering phenomena and relies heavily on the integration of computational fluid dynamics (CFD) and finite element methods (FEM).

FSI is particularly valuable in industries such as automotive, aerospace, maritime, civil, and biomedical engineering. By incorporating both fluid and structural mechanics, it enhances the reliability and accuracy of simulations, providing engineers with a comprehensive understanding of the system. Numerical methods that couple CFD and computational structural mechanics (CSM) are employed to study complex behaviors, including aeroelasticity, aeroacoustics, vibrations, structural fatigue, and flow instabilities. This approach ensures components are designed to be robust and reliable for their intended applications.

1.2 Purpose

We recognized an exciting opportunity to use fluid-structure interaction (FSI) as a learning tool to design and manufacture a carbon fiber composite rear wing for our Formula Student car. This project allowed us to not only aim for a high-performance vehicle but also ensure that every component is efficient and safe. As part of this effort, we decided to move away from the traditional hand layup method and instead try a new type of carbon fiber prepreg. This gave us a chance to explore a more advanced and precise manufacturing technique that could improve the overall quality and performance of the wing.

The integration of FSI-based simulations was particularly valuable as it allowed us to analyze the dynamic interaction between aerodynamic forces and the structural response of the rear wing. By simulating airflow patterns, pressure distributions, and resulting deformations, we were able to maximize downforce while minimizing drag with the appropriate wing geometry. This approach ensured that the wing delivers optimal aerodynamic performance under racing conditions, contributing significantly to vehicle stability and cornering efficiency. Finally, the purpose of conducting these simulations was also to validate our rear wing's design and safety compliance, as it is not only the vehicle but also the driver's safety that we need to consider.

1.3 Goals

Building on the purpose of designing a high-performance rear wing, our goals are clearly defined to ensure measurable and impactful outcomes. These objectives guide our design and development process and serve as benchmarks for evaluating our success:

- **Increase Downforce for Enhanced Grip:** Design the rear wing to generate higher downforce, improving the overall grip of the car. This enhancement not only benefits cornering but also provides greater stability during acceleration. Increased downforce is expected to significantly reduce lap times in various events such as the Acceleration, Skidpad, and Autocross events, as well as the most critical high-scoring events: Trackdrive and Endurance.

- **Enhance Stiffness and Stability:** Optimize the structural design of the rear wing to ensure high stiffness and stability under dynamic conditions with significant pressure differences. By minimizing deformation, the airfoil profile and rear wing geometry will remain intact, preventing loss of traction and maintaining cornering efficiency. This objective focuses on ensuring consistent aerodynamic performance without compromising the reliability of the component during competition.

- **Explore New Manufacturing Techniques:** Investigate and implement a new prepreg manufacturing process, along with exploring advanced composite materials for the carbon fiber and core. This will improve the quality of the rear wing while also reducing manufacturing time. By experimenting with innovative materials and processes, the objective is to achieve higher precision and durability in the final component.

- **Validate the Design through FSI Simulations:** Conduct FSI simulations to validate the rear wing design for compliance with the Formula Student Germany Rulebook [2]. Specifically, ensure that the aerodynamic device does not deflect more than 10 mm in the load-carrying direction when subjected to a load of 200 N over a minimum surface area of 225 cm^2. This step is crucial for both regulatory compliance and the reliability of the design under competitive conditions.

These goals are designed to push the limits of performance, safety, and innovation, aligning with the competitive standards of Formula Student while fostering practical learning and application of advanced engineering techniques.

1.4 Limitations / Assumptions

Some of the main limitations/assumptions that we had are as follows:

- The design validation was specifically targeted for compliance with the Formula Student Germany Rulebook. Adaptations for other competition rulebooks or future regulatory changes were not considered.
- The project was restricted to the carbon fiber prepreg and PVC foam core materials available in our inventory. Exploring alternative materials was beyond the scope of this work due to resource limitations.
- The aerodynamic study focused on optimizing downforce and drag under competition-specific conditions. Broader investigations, such as the effects of wind sensitivity or multi-vehicle interactions, were excluded.
- The project timeline, bound to the Formula Student season, limited the extent of iterative design improvements and exploration of alternative solutions.
- Due to limited computational resources and time, the CFD simulations utilized a coarser mesh for the wind tunnel, except in critical regions around the rear wing where finer meshing was necessary for accuracy.
- The creation of multiple geometries was required to accommodate different software programs, such as Star CCM+ and Ansys Fluent for CFD, and Ansys ACP for structural and composite FEM analyses. Preparing these geometries, including volume mesh for CFD, surface geometry for FEM and ensuring appropriate contact surfaces for the composite simulations, was time-intensive and restricted the pace of the design process.
- The project scope was influenced by available computational power, software capabilities, and team expertise, which set practical limits on the complexity and scale of simulations and analyses.

2

Theory

In the following sections, we talk about some important concepts considered during this project.

2.1 Aerodynamics

Airfoils are aerodynamic devices that generate lift or downforce (negative lift).Their main function is to provide a reduced resistance to incoming air flow. They do this by guiding the air over the leading edge and in turn reducing the turbulent wake behind the airfoil. The degree of its perrformance is characterised by a number of parameters, such as chord length, angle of attack, airfoil shape in general, camber, etc.

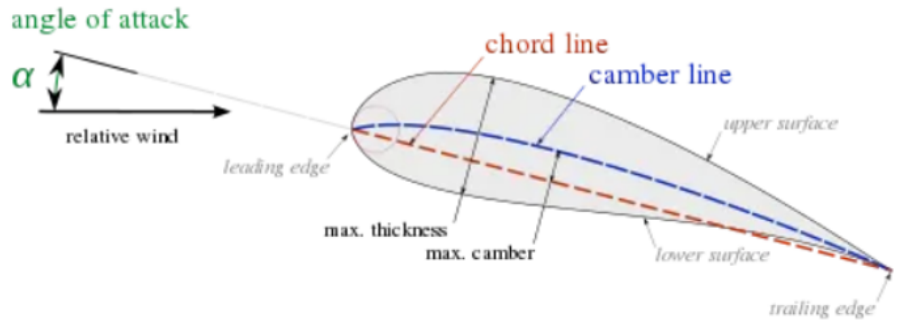

Figure 2.1: Airfoil nomenclature

Depending on the type of application, these parameters are altered in order to optimise performance. In this case, two main airfoils were quickly analysed to be used at the rear-wing flaps, and $S1223$ was chosen because they largely operate over higher Cl values across a range of $AoAs$, and do not have a steep stall angle.

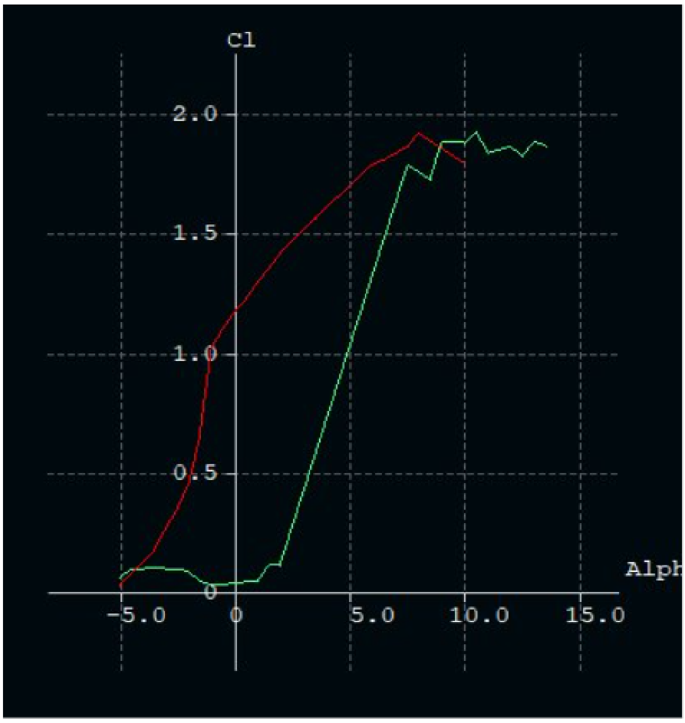

Figure 2.2: Cl vs α for $S1223$ (red) and $MSHD$ (green)

Dynamics parameters such as the AoA on a flap play a crucial role in performance. If the pressure recovery is too high, flow reversal will occur, leading to separation. This is characterised by a recirculation of fluid flow in this region where there is an increase in drag and loss of total pressure.

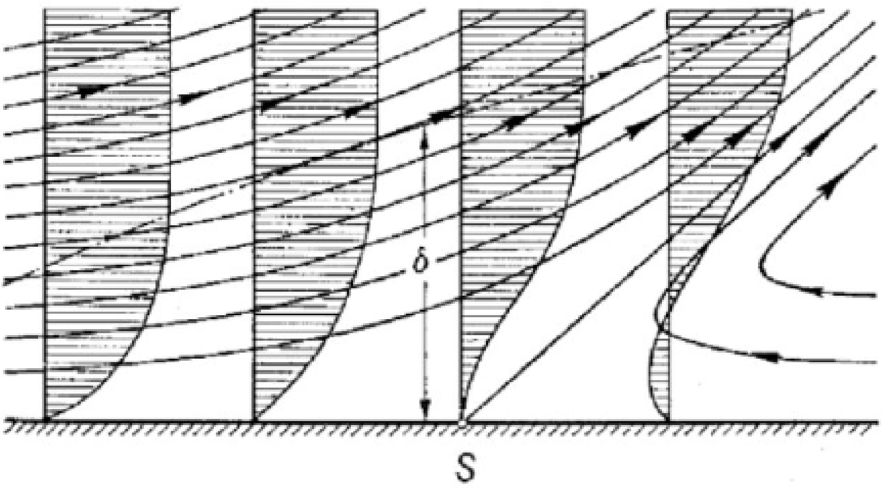

Figure 2.3: Flow reversal

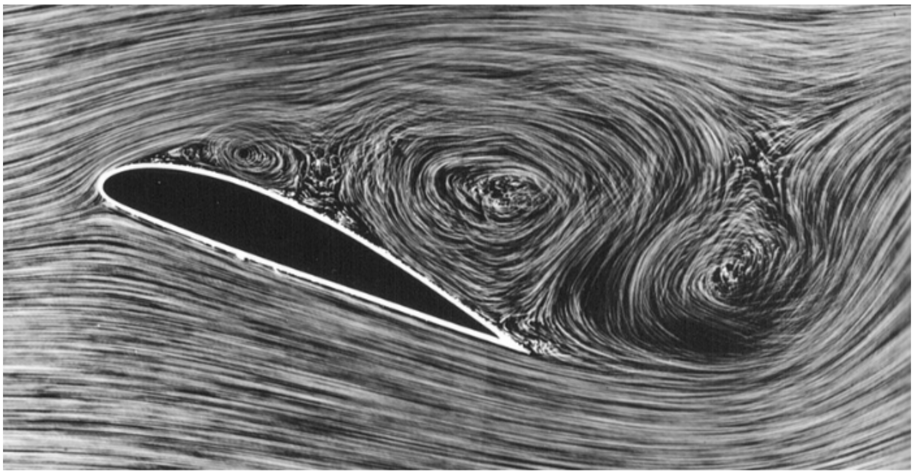

Figure 2.4: Airflow separation from airfoil as characteristic in stall [1]

2.1.1 Aerodynamics in Formula Student

In the formula student competition, the goal is basically to build an open-wheel, formula-like race car. There are some rules regarding aerodynamic devices, not as strict as in higher racing categories but we also have bounding boxes where the device can be can not extend more, but in this box there is freedom to basically do whatever you want. From the lap time simulator, we have come to the conclusion that the most important thing is downforce, that is why the wings look large compared to the car. In this study we want to investigate how much does the wing deforms under significant speed achieved. This speed can be achieved for example on the long straight, or during the acceleration discipline.

2.2 Composites

Composites are materials formed by combining two or more distinct materials, each with unique physical and chemical properties, to produce a material with superior overall characteristics compared to the individual materials. Composites are generally classified into two main components: the matrix and the reinforcement. The matrix binds the reinforcement, providing structure and enabling the desired mechanical properties, while the reinforcement provides the strength and stiffness to the material.

Composites are highly valued for their excellent strength-to-weight ratio, making them indispensable in industries such as automotive, aerospace, and sports. Common types of composites include glass fiber reinforced polymers (GFRP), carbon fiber reinforced polymers (CFRP), and aramid fiber composites. In this project, we will focus on a sandwich CFRP composite, which consists of carbon fiber as the stack-up with a PVC core material, forming a lightweight, strong, and durable structure.

2.2.1 Structure and Components of Composites

The structure of composites plays a significant role in determining their mechanical performance. In this section, we will outline the components and structure of our specific composite setup.

2.2.1.1 Carbon Fiber

Carbon fiber is produced from organic polymers, primarily polyacrylonitrile (PAN), which makes up about 90% of carbon fibers. The remaining 10% of carbon fibers are produced using either rayon or petroleum pitch. These fibers are composed of long molecular chains bonded together by carbon atoms to maximize strength. The fibers are often woven into fabrics, and different weave patterns, tow sizes, and fiber grades influence the mechanical properties of the final composite. We can see the types in Figure 2.5.

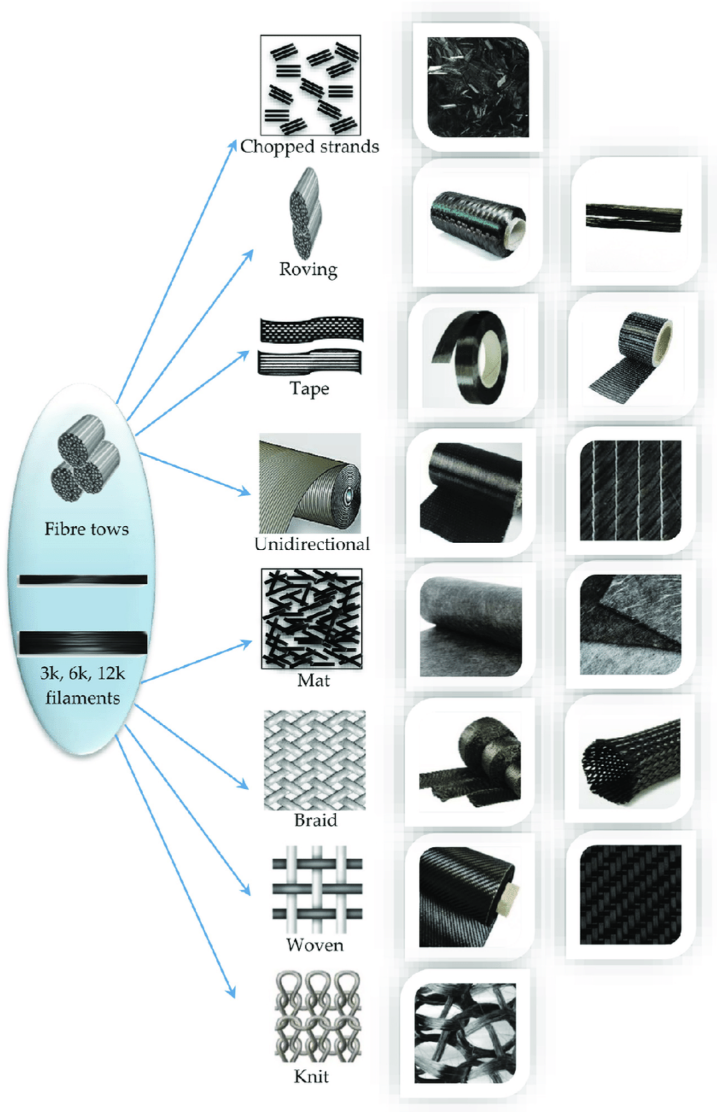

Figure 2.5: Different types of Carbon Fibers

The most common weave patterns used in industry are unidirectional, plain weave, and twill weave. For this project, we will be using "twill weave carbon fiber." Specifically, we will utilize an "Epoxy Carbon Fiber Woven Prepreg (230 GPa)" from the Ansys composite material library for our simulations.

2.2.1.2 Prepreg Materials

Prepreg refers to fiber sheets that have been pre-impregnated with a resin, usually epoxy, before being used in manufacturing. The resin is evenly distributed throughout the fiber mat, ensuring uniform mechanical properties. This method significantly reduces human error during the layup process and ensures a more consistent resin distribution around the fibers. The image of the fiber is shown in Figure 2.6.

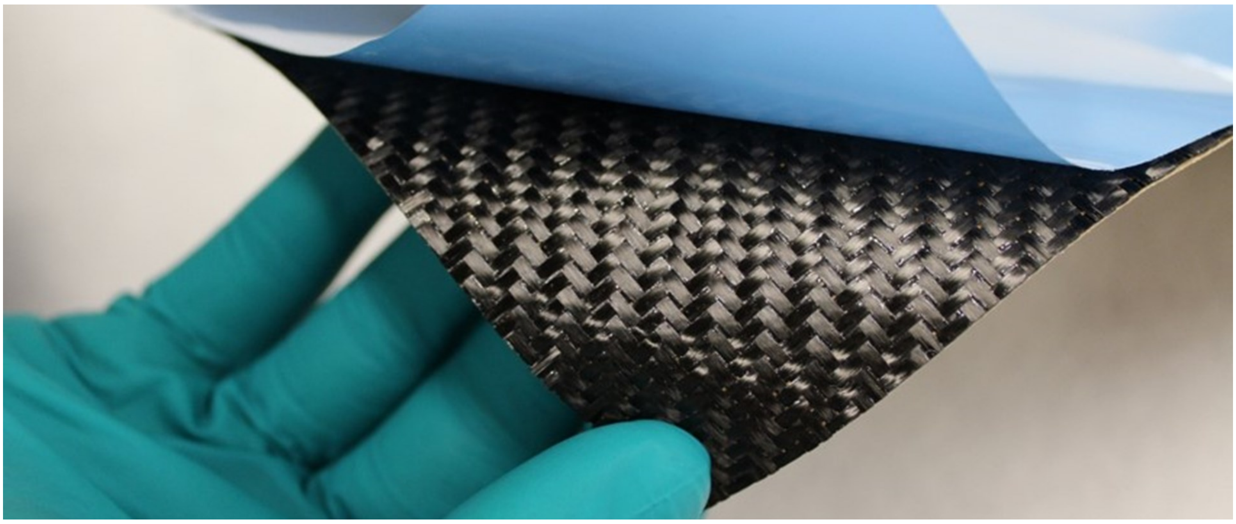

Figure 2.6: Twill Weave Prepreg

In our case, the prepreg sheets are made of carbon fiber, and once laid up onto the mold, they must undergo a curing process under vacuum and in an autoclave to fully cure the resin and achieve the desired material properties. This process ensures proper consolidation of the fibers and resin, resulting in a high-performance, durable component.

2.2.1.3 Sandwich Structure

We are using a "PVC foam core (60 kg/m^3)" sourced from the Ansys composite material library. The combination of the carbon fiber prepreg and the PVC foam core forms a sandwich structure, which is known for its excellent strength-to-weight ratio. This setup provides stiffness and durability while maintaining a light weight, making it ideal for high-performance applications such as our Formula Student rear wing design. The sandwich structure plays a critical role in ensuring that the component can withstand the dynamic loads and aerodynamic forces that will be applied during racing. We can see how the sandwich panel looks in the Figure 2.7.

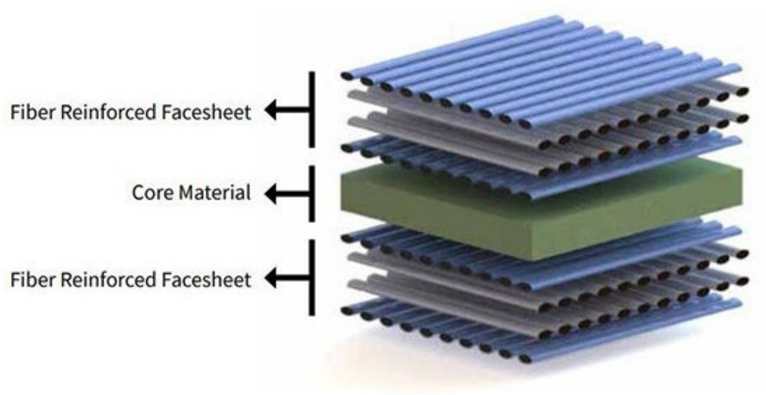

Figure 2.7: Sandwich Composite Panel

2.2.2 Advantages of Composites

Composites are particularly advantageous for applications where high strength-to-weight ratios are required. In automotive applications, such as Formula Student, reducing the weight of components while maintaining or improving strength and performance is essential for optimizing the vehicle's overall efficiency and speed.

Another significant advantage of composites is their ability to be molded into complex geometries. This allows for highly customized and optimized designs tailored to the specific needs of the application. Moreover, composites are highly resistant to corrosion and degradation under various environmental conditions, making them suitable for use in a wide range of climates, including hot summers, rainy conditions, and cold winters.

Furthermore, composites are known for their resistance to fatigue. They maintain their structural integrity and performance even under repeated loading cycles, making them ideal for dynamic applications like motorsports.

2.2.3 Limitations of Composites

Despite the numerous advantages, composites do have some limitations. One major drawback is the high initial cost of manufacturing, both in terms of the materials and the production setup. Composites require specialized equipment and expertise, which can increase the upfront costs.

Additionally, the manufacturing process can be complex and labor-intensive, which may result in material waste and production delays if not managed properly. Moreover, composites can be prone to defects, such as delamination or voids between layers, which can significantly reduce the strength of the final product if not properly addressed during manufacturing.

2.2.4 Relevance to Formula Student

In the context of Formula Student, composites play a crucial role in enhancing vehicle performance by reducing the weight of critical components. Components such as the rear wing, monocoque, and aerodynamic devices rely heavily on composites for their strength and stiffness, particularly under dynamic loads encountered during racing events.

For Formula Student teams, the ability to optimize the balance between weight reduction and structural integrity is essential to achieve the best performance within the strict weight and safety constraints of the competition. The use of CFRP in components like the rear wing allows teams to achieve maximum aerodynamic efficiency and durability while keeping the weight low, which ultimately contributes to improved lap times and overall vehicle performance.

3
Methods

The CFD simulation was done in Ansys Fluent which had to switch to after we did it in Star-CCM+ because we wanted to couple the structural simulation which was done in ACP and we could not find a way to couple it with Star CCM+. In Fluent, we established the mesh 60 mm base size and refinements on the whole wing geometry. For the solver we used $k - \omega\ SST$ model with a built-in wake model to better resolve the wake. Boundary conditions were 100 km/h flow velocity. This flow velocity was chosen because we wanted to have higher stress from the pure aerodynamics, because even though the wing itself experiences this conditions in very few occasions we wanted to showcase the durability of the wing in these extreme aerodynamic loads. Because as we mentioned this is very off-design case you can see that the wing aerodynamic performance is not optimal in this condition.

3.1 STAR-CCM+

3.1.1 Simulation setup

This section describes the simulation setup in STAR-CCM+. Though ANSYS was used as the coupling software, the results obtained from $STAR$ helped validate the accuracy of our ANSYS setup to a certain extent.

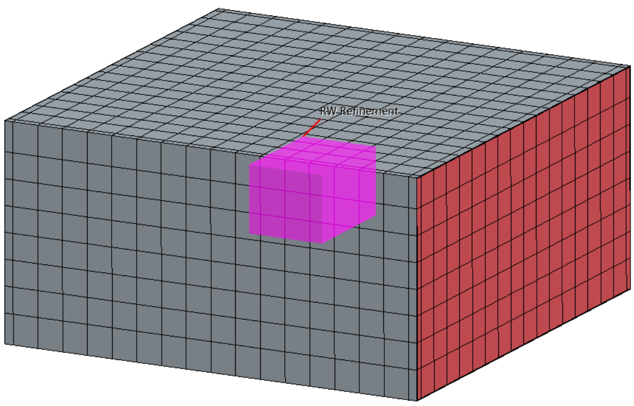

Figure 3.1: Refinement box around the rear wing

The refinement box around the rear wing was made to create a finer mesh around the body so that the fluid flow around it can be captured accurately, especially the suction and pressure sides of the flaps, and the wake regions.

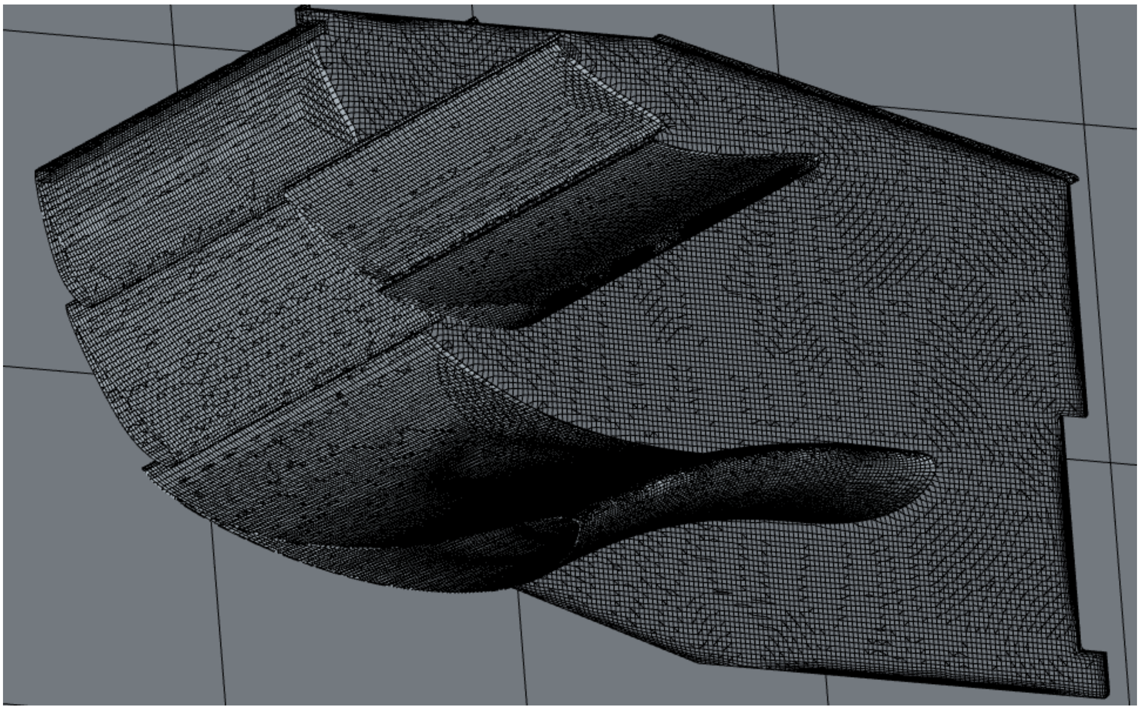

Figure 3.2: Refined rear wing mesh

3.1.2 Results

The simulation was run for a 1000 iterations for reasonable convergence. The negative lift (downforce) generated by the rear wing was monitored and plotted; we could see that value obtained was ≈ 954 N.

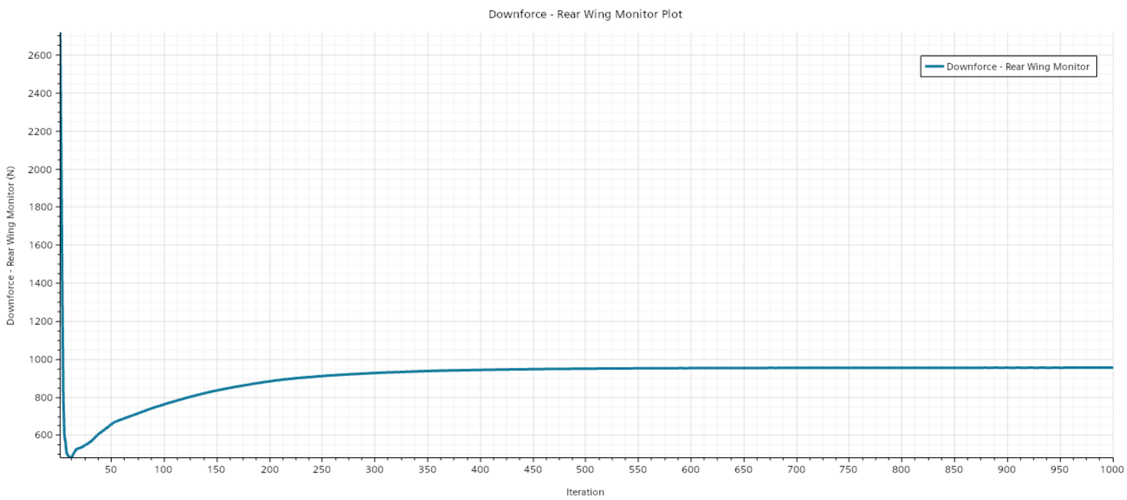

Figure 3.3: Rear wing downforce monitor

To further understand and validate the physics, scalar scenes for pressure (see figure 3.4) and velocity (see figure 3.5) were made.

Figure 3.4: Static pressure scalar scene

The static pressure scalar scene indicates a clear pressure gradient between the suction and pressure side of the flaps, i.e., a region of low pressure on the suction (lower) side and higher pressure on the pressure (upper side).

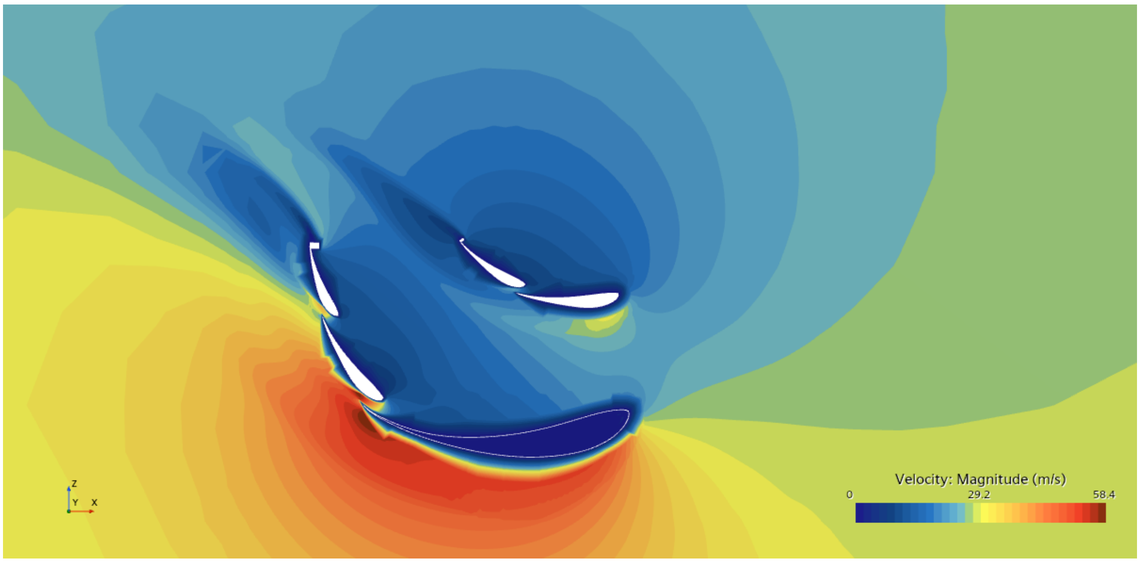

Figure 3.5: Velocity scalar scene

As expected, the velocity scalar is in accordance with the pressure regions in the sense that the velocity of flow is higher on the suction side and vice versa on the pressure side.

3.2 ANSYS ACP

We will be using ANSYS ACP and Static Structural applications for our FEM Analysis. We have chosen this particular application as ACP enables us to model composite structures and perform FEM on that particular component. We will now discuss the method and workflow adapted for our project.

3.2.1 Geometry and Meshing of the Rear Wing

According to the requirements of ANSYS ACP, a shell model was utilized for the composite layup, as it closely mirrors the real-life structure of the wing. To achieve this, a surface model of the rear wing was created and divided into seven segments: Overwing 1, Overwing 2, Overwing 3, Overwing 4, the Main Segment, and the Right and Left Endplates, as illustrated in the Figure 3.6. These segments were assigned as named selection sets for subsequent use in the simulation.

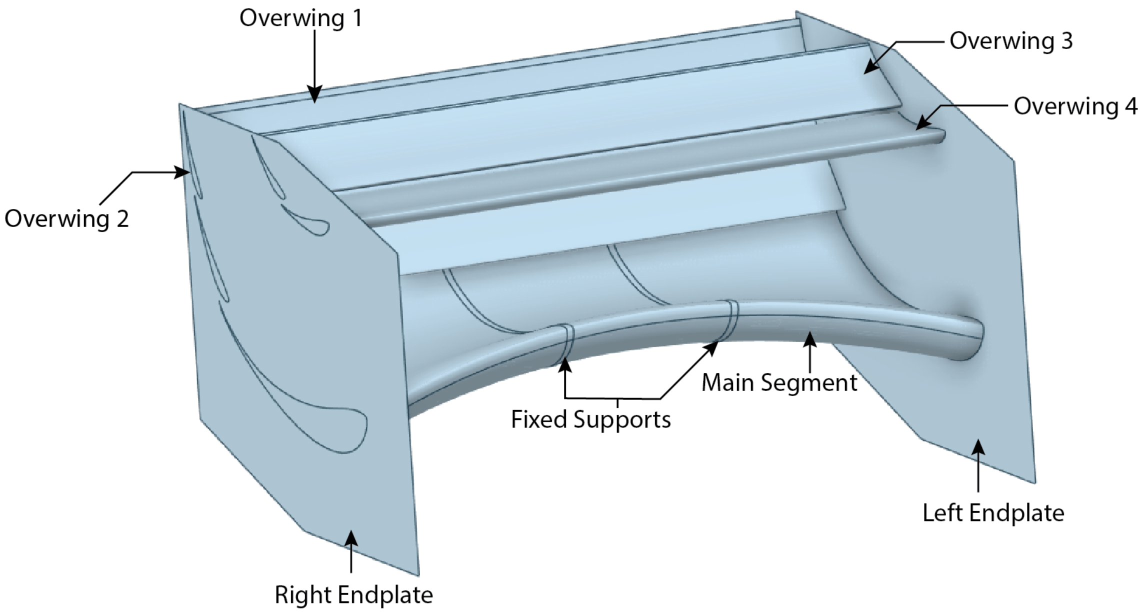

Figure 3.6: Geometry Definition of the Rear Wing

The image above shows the surface model of the rear wing in ANSYS SpaceClaim. Since the rear wing will incorporate an attachment bracket, the surface area within the main segment where the bracket will be positioned was also defined. This surface serves as the fixed support for the simulation, while in real-life conditions, an aluminum bracket fastened to the main hoop bracings of the car will be used.

Once the surface model was finalized, the meshing process was carried out in ANSYS Mechanical. The maximum element size was set to 3 mm to maintain a balance between computational efficiency and solution accuracy. Additionally, the Automatic (PrimeMesh) method was employed, utilizing a quadrilateral-dominant shell mesh type. This approach produced a fine mesh, ensuring precise results, as shown in the Figure 3.7. The mesh quality was particularly fine near the leading and trailing edges of the wing profiles. In total, the mesh comprised 568,211 elements.

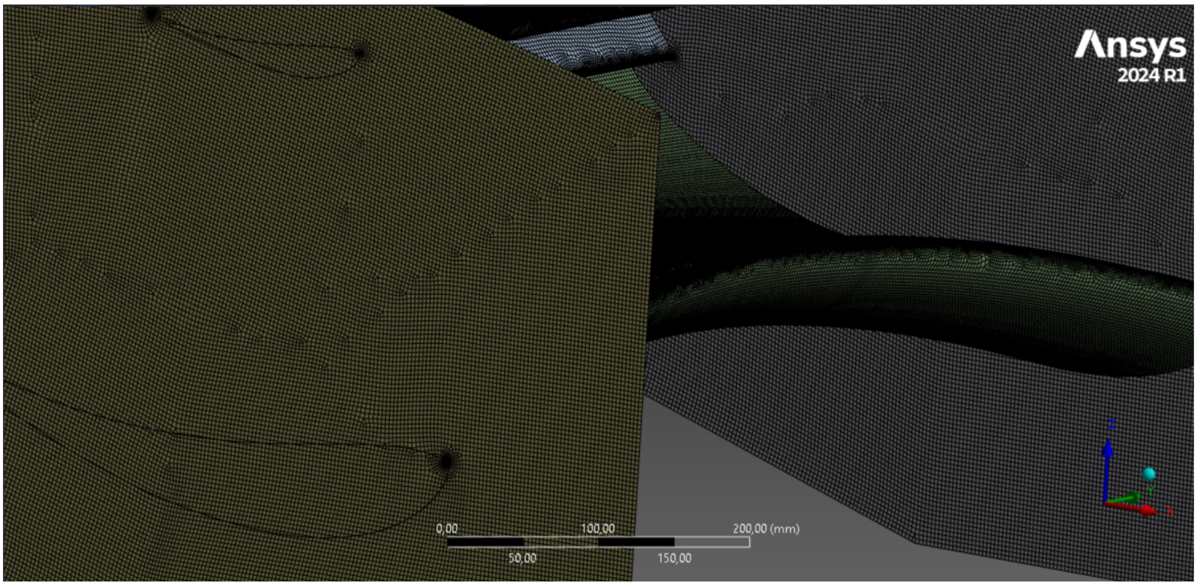

Figure 3.7: Closeup View of the Mesh For ACP and FEM analysis

3.2.2 Setup For *ACP*

Firstly, the fabrics and their respective thicknesses were defined, and a stackup was created for the composite layup. This stackup adopts a sandwich composite structure, which incorporates a core material sandwiched between layers of carbon fiber. A sandwich composite can be described as having a "top skin," a "core," and a "bottom skin." The top and bottom skins consist of carbon fiber layers, while the core is made from a lightweight material. This structure is particularly advantageous in our case, as it significantly reduces the overall weight of the aerodynamic package while enhancing the bending stiffness of the laminate. The inclusion of the core material ensures greater stiffness compared to a monolithic carbon fiber laminate, improving performance under bending loads.

The top skin of the structure consists of three carbon fiber layers oriented at 0°, −45°, and −90°. The core is a 5 mm PVC material, followed by three additional carbon fiber layers in the bottom skin, oriented at 90°, 45°, and 0°. These orientations are critical as they determine the distribution of strength in various directions of the laminate. The cross-sectional view of the sandwich laminate is shown in Figure 3.8. In this image, “a” denotes the angle of orientation, while “t” represents the thickness of each layer. The polar properties of the composite structure, shown alongside, highlight the mechanical properties:

- $E1$: The longitudinal modulus of elasticity, representing stiffness along the primary fiber direction (1-direction).
- $E2$: The transverse modulus of elasticity, representing stiffness perpendicular to the fiber direction (2-direction).
- $G12$: The in-plane shear modulus, which describes the material’s resistance to shear deformation in the plane of the laminate (1-2 plane).

The polar diagram indicates how these properties vary with direction, with peaks near the 90° multiples. Their respective strength values, measured in Pascals (Pa), are provided in the accompanying image.

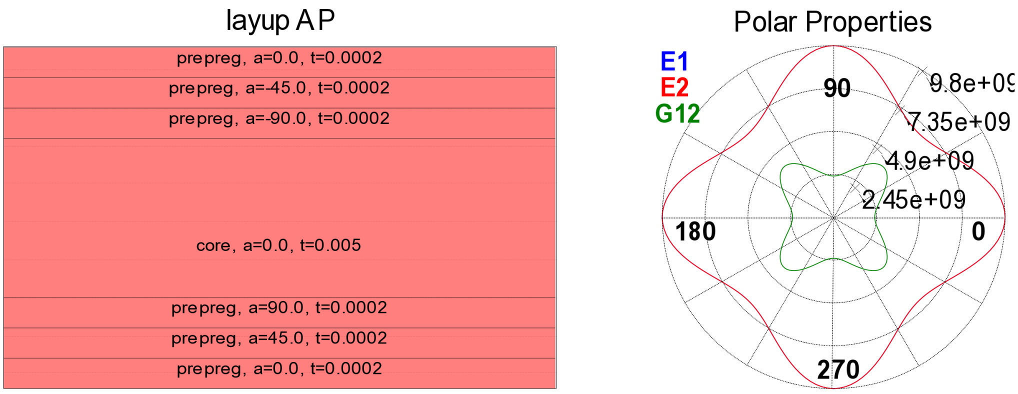

Figure 3.8: Cross-sectional view of the sandwich laminate and polar properties.

3.2.3 Oriented Selection Sets

Next, the oriented selection sets were defined to ensure the correct fiber thickness direction with regards to their appropriate rossette direction. The fibers were configured to build thickness inward to maintain the intended geometry. This setup aligns with the layup process, where negative molds are used to shape the structure. In this step, the thickness direction of the fibers was verified, and arrows on the main segment pointing inward (Z-direction) were observed, as shown in Figure 3.9. This step ensures that the layup direction matches the design intent and the mold setup.

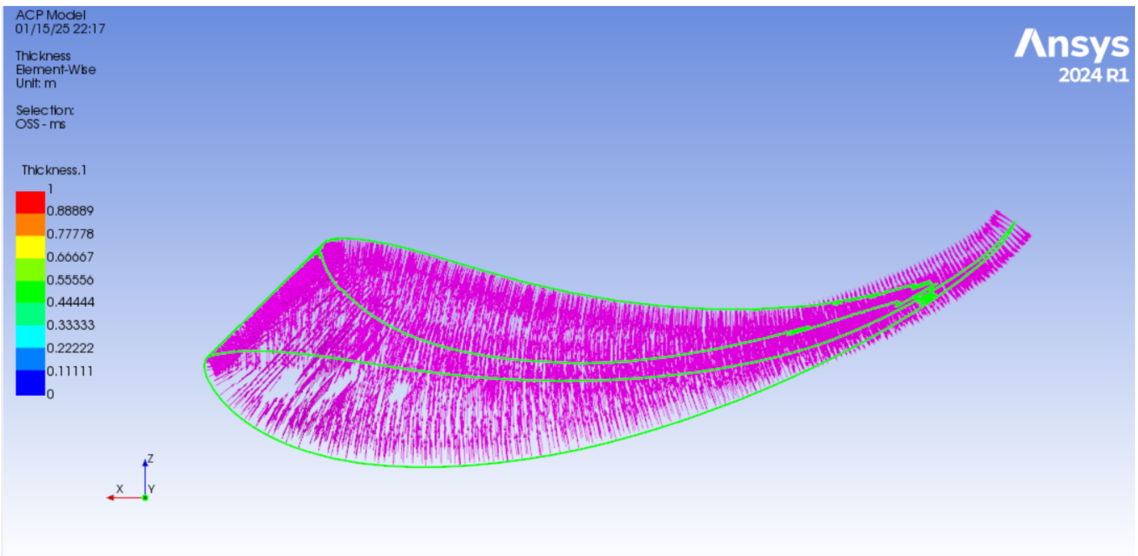

Figure 3.9: Definition of thickness direction for the layup.

3.2.4 Layup Application and Verification

Subsequently, the layup was applied to all wings and flaps. The X, Y, and Z directions of all layers across the structure were verified. An example of this verification on the right endplate of the rear wing is shown in Figure 3.10. Upon completing these verifications, the ACP (Ansys Composite PrepPost) setup was finalized, enabling us to proceed to the static structural analysis. In this next phase, boundary conditions for the CFD and FEM analysis will be defined.

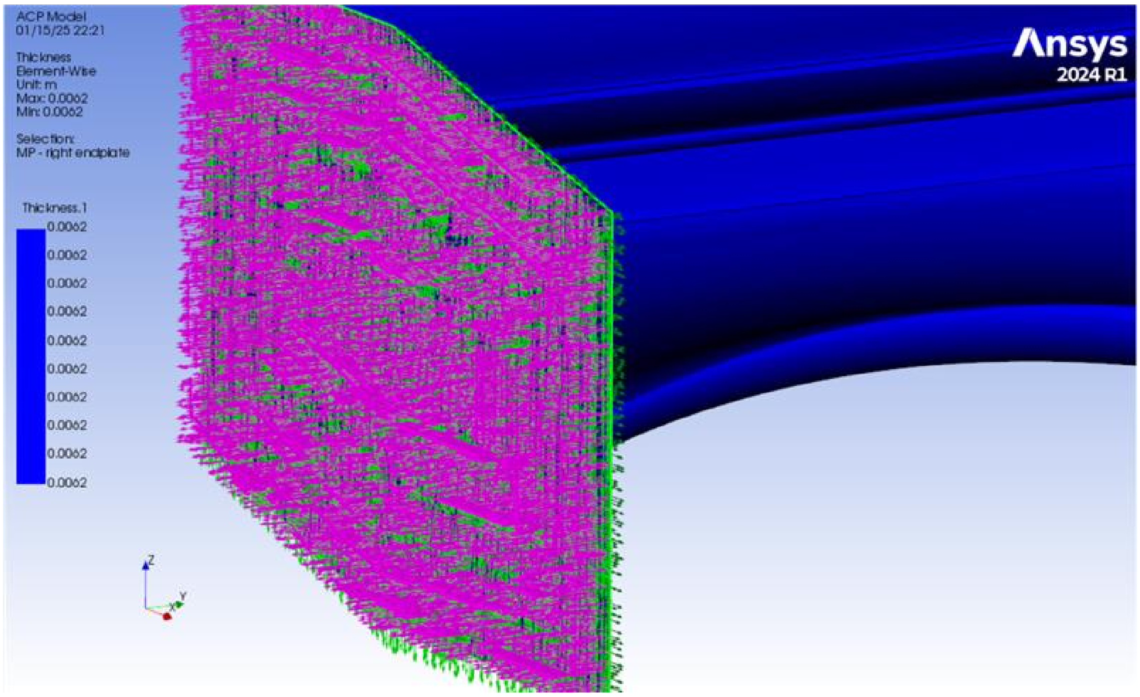

Figure 3.10: Verification of X, Y, and Z directions of the layup on the rear wing right endplate.

3.3 ANSYS Fluent

Apart from the details mentioned in the coming sections. Further details regarding setup and solutions are mentioned in the form of a solution report in the appendix.

3.3.1 Boundary Conditions

Standard boundary conditions of a velocity inlet with a velocity magnitude of 27.78 m/s which translates to 100 km/h and pressure outlet were used as indicated by the blue and red arrows respectively on the wind tunnel face in figure 3.11.

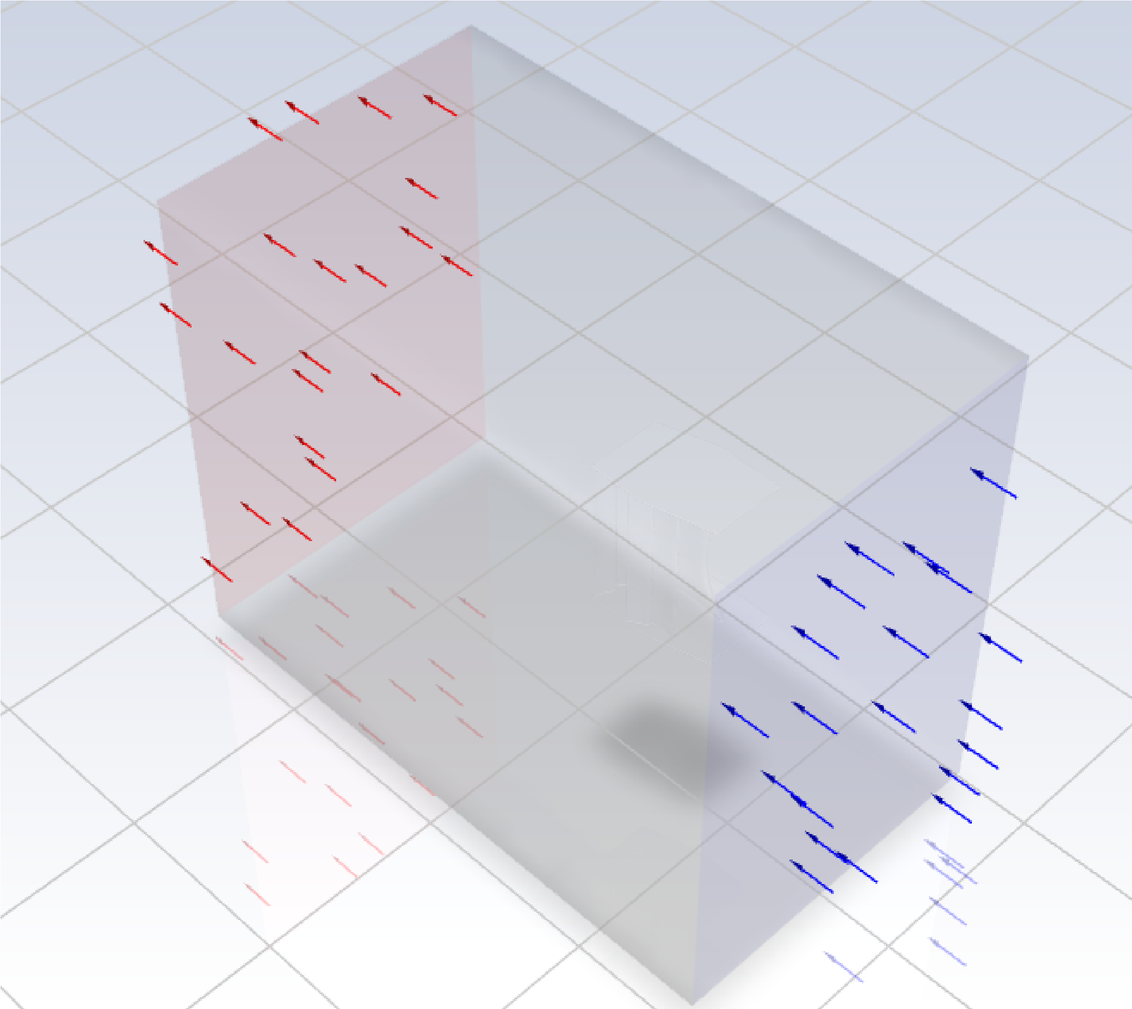

Figure 3.11: Fluent setup

For the viscous model $k - \omega$ SST model was chosen. The simulation is low speed, incompressible, and for the transition model to resolve the wake better, γ transport equation model was chosen. Apart from the inlet and outlet, we applied slip condition on the other walls as we are just isolating the wing and focusing on the pure aerodynamic sources, and to make less demand on the computational power. We assumed standard atmospheric conditions at sea level so temperature 288.16 K and 1.225 kg/m3 air density. We also needed to find out the frontal area, which we did in the 3D modeling software Siemens NX.

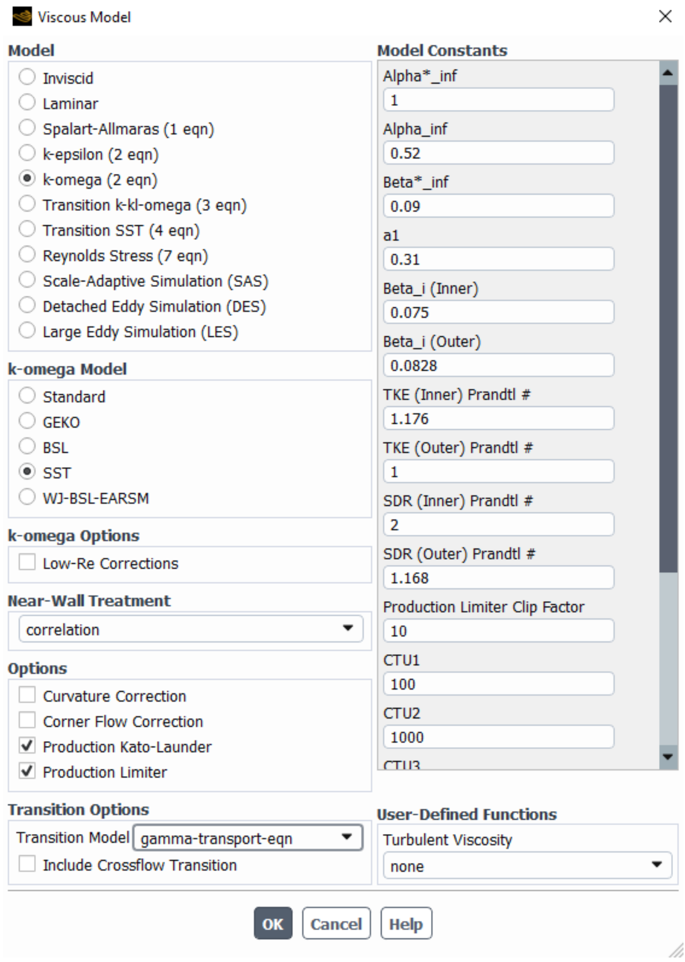

Figure 3.12: Viscous model

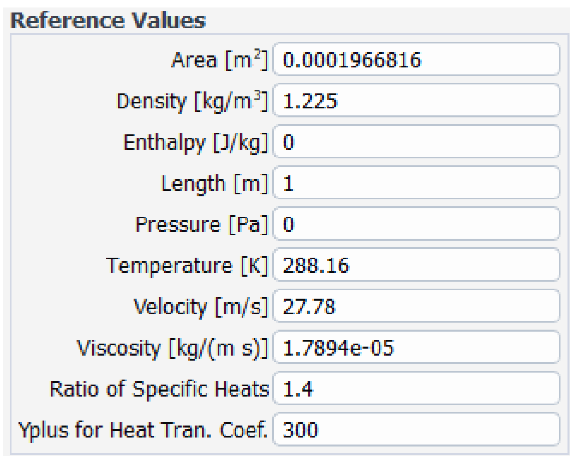

Figure 3.13: Reference values

3.4 Software Coupling

In this step, we couple the *ACP* and Fluent modules to perform a comprehensive FEM analysis. This coupling enables the integration of aerodynamic data obtained from the Fluent module with the composite plies defined in ACP, thereby ensuring accurate and realistic simulation results. The Static Structural module facilitates this coupling by importing the relevant pressure data and defining the load cases.

We can see the complete workflow and coupling system in the following Figure 3.14:

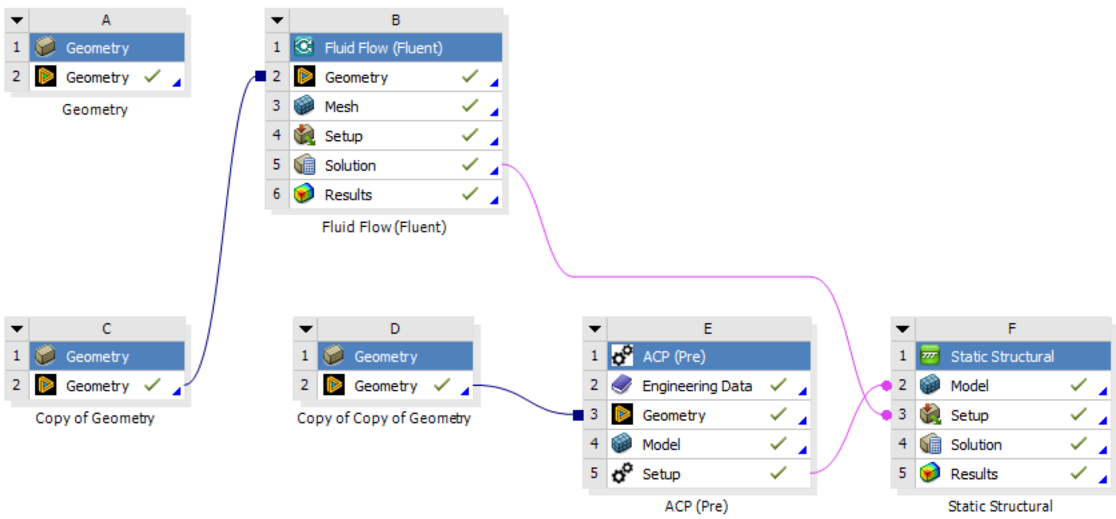

Figure 3.14: Software coupling

3.4.1 Boundary conditions and Setup

The boundary conditions were defined using the pressure data imported from the Fluent module. This aerodynamic pressure data represents the load case applied to the rear wing and is critical for assessing the structural performance of the wing under operational conditions. The applied pressure distribution is visualized in the Figure 3.15

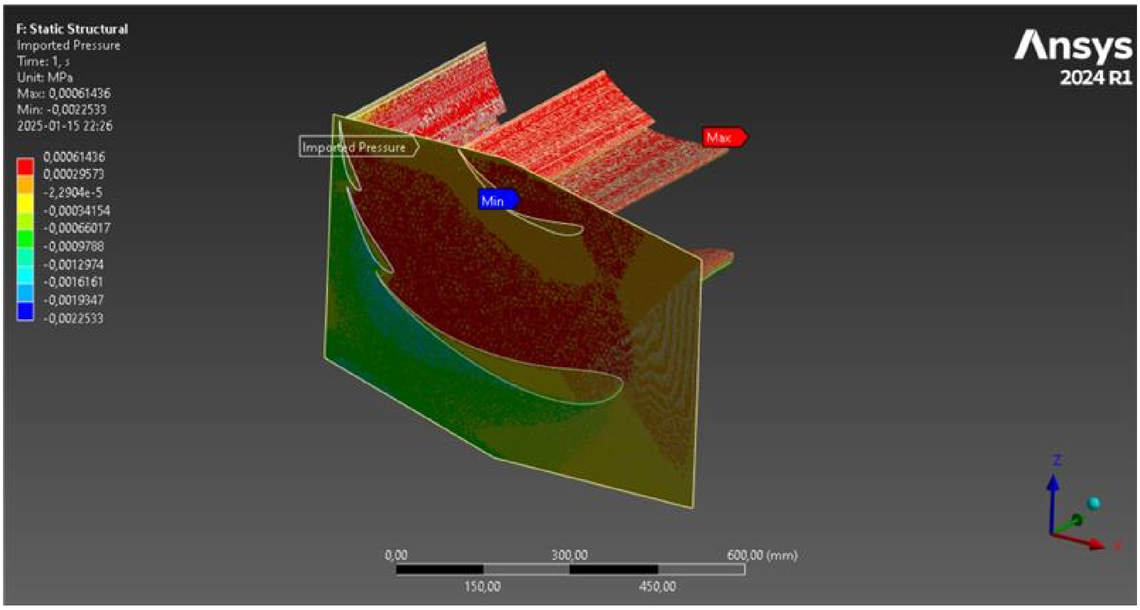

Figure 3.15: Pressure Load Imported from Fluent into Static Structural

Additionally, the rear wing requires a fixed attachment point to simulate its mounting on the vehicle. For this purpose, we used the named selection set designated as "fixed" to define the fixed boundary conditions. These elements correspond to the area where the wing will be attached to the vehicle. The fixed boundary condition is shown in the Figure 3.16

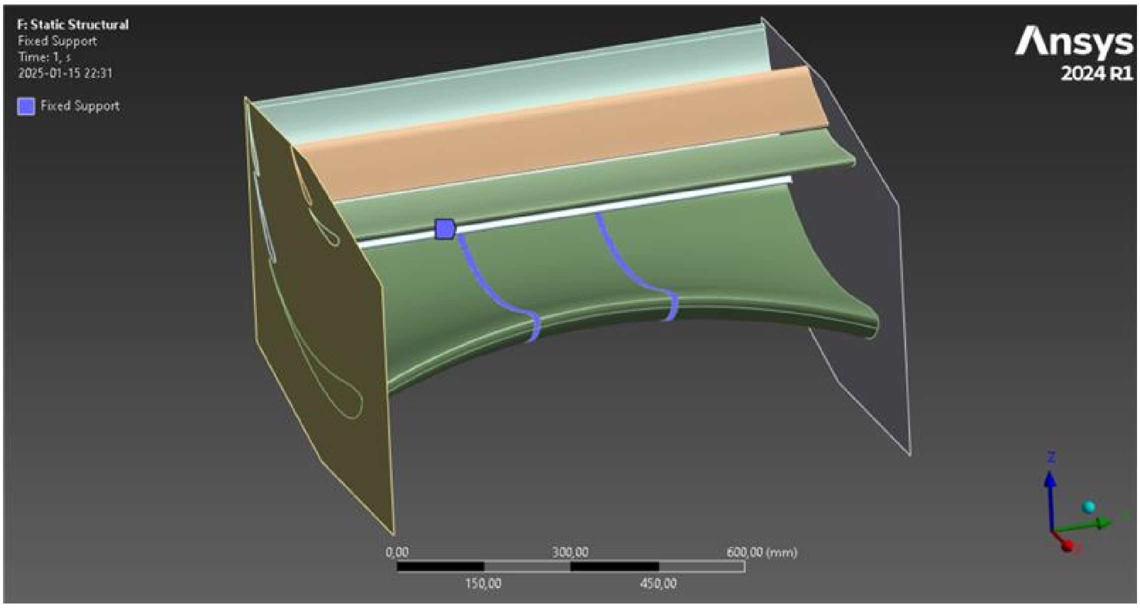

Figure 3.16: Pressure Load Imported from Fluent into Static Structural

While the setup process might appear straightforward, it required meticulous verification to ensure the accuracy of the imported data. In some instances, the process encountered errors, causing interruptions to the solutions. This made the task significantly more challenging and time-intensive than it initially seemed.

4

Results

From the CFD analysis we managed to get very similar results although we believe that the CFD results from Star CCM+ might be more accurate because we did not manage to implement the prism layers in the Ansys Fluent CFD simulation due to the complexity of the meshing and also time demands.

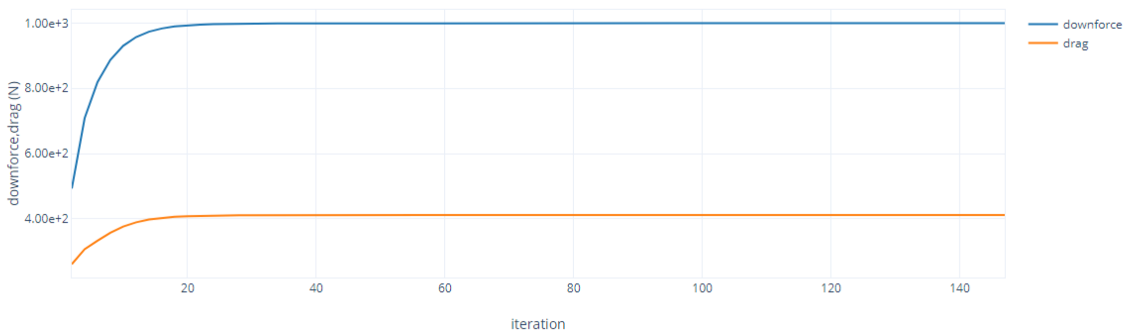

Figure 4.1: Downforce Monitor plot

From figure 4.1, we can see that the downforce stabilizes close to 1000 N, (999.5239 N), which is quite close to what was obtained on STAR.

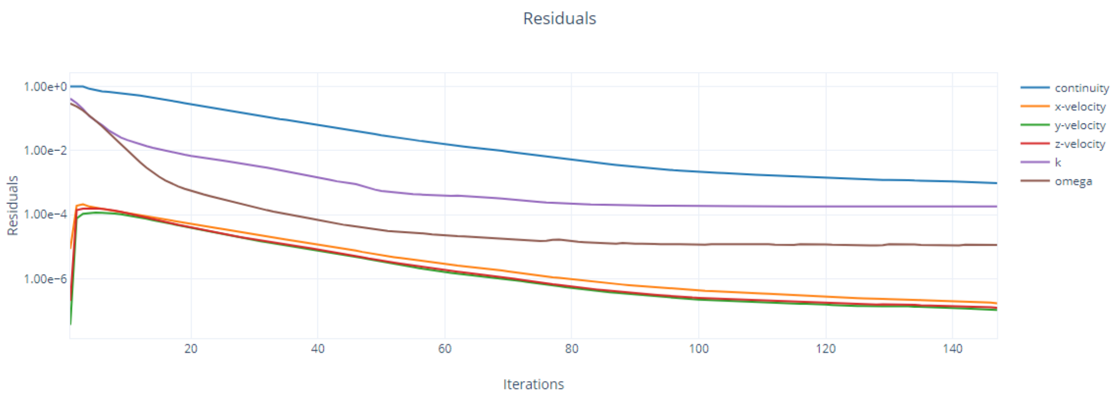

Figure 4.2: Residuals

As can be seen from figure 4.2, the solution converges after 147 iterations.

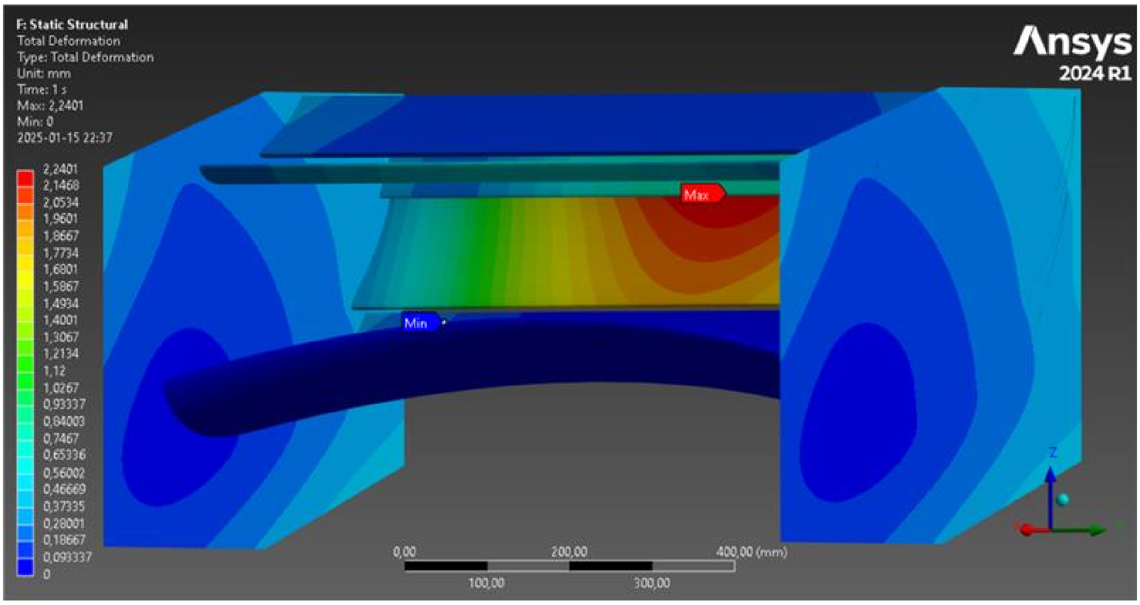

Figure 4.3: Deformation of the Rear Wing in True Scale

Figure 4.3 shows the deformation in different elements of the rear wing. The minimum point of deformation is shown to be on the main segment. This is understandable as the mounting point of the rear wing on the formula student car is typically via the main segment i.e., fixed support with the help of mounting supports, therefore already experiencing a level of rigidity. The maximum deformation is 2 mm at a point on the overwing; this is due to the large pressure gradient between the suction and pressure side of the flap when travelling at 100 kmph.

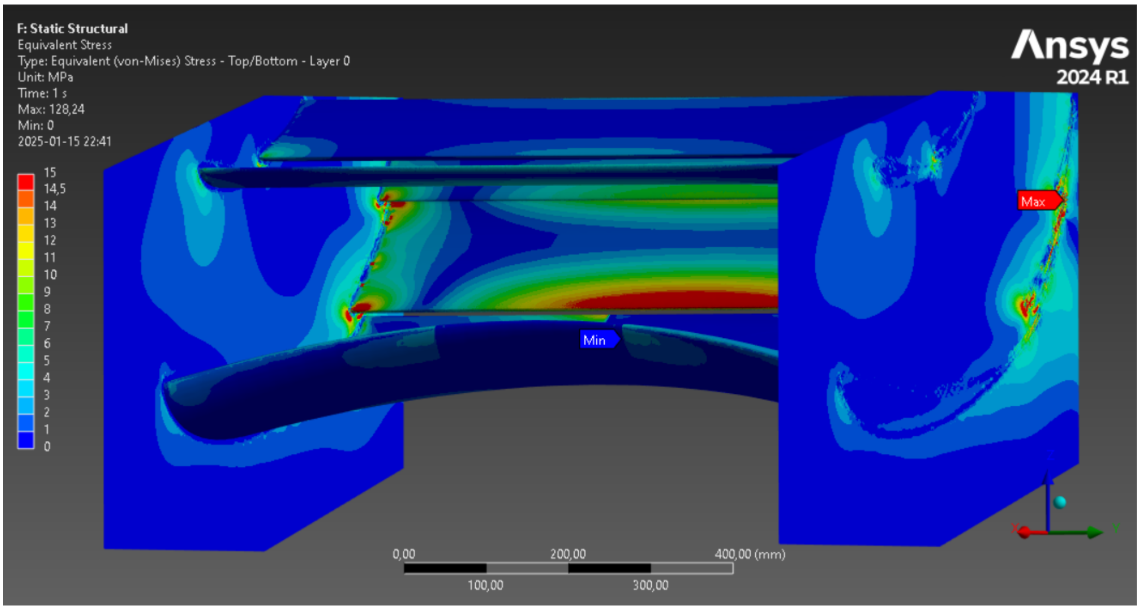

Figure 4.4: Equivalent Stress on the Rear Wing

Understanding the type and magnitude of stresses occurring on the component is of great importance as it tells us if there is a weak spot/design flaw in the body.

Typically, a stress tensor is described by a 3 x 3 tensor representing both tangential and normal stresses. This is where equivalent stresses are useful as they combine these nine values into one scalar value, giving us a holistic picture.

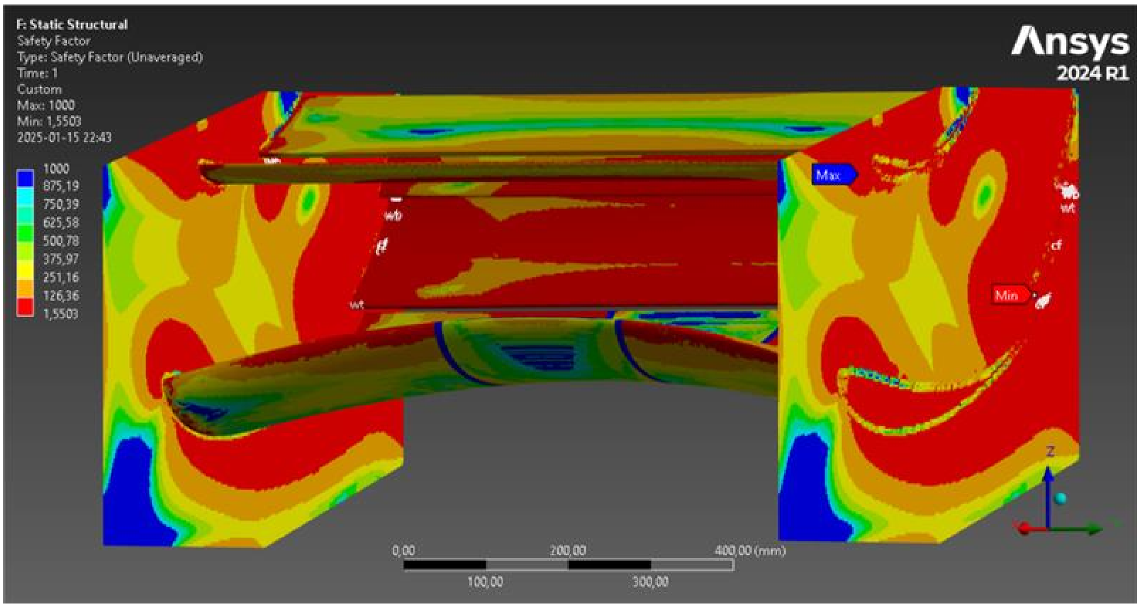

Figure 4.5: Safety Factor of the rear wing

The minimum factor of safety measured came out to be about, $1.5 - 2$ and these values were observed near a node or a singularity while the surrounding elements near that node had a high safety factor value; hence, we can deem this design to be safe to operate under our racing conditions. The segment between the fixed support seems to have a larger safety factor, and once again, this is due to the rigid mounting points.

5

Conclusion

The objective of this project was to study the fluid-structure interaction (FSI) on the rear wing of a Formula Student race car and assess its effect on aerodynamic performance. To achieve this, we conducted numerical simulations using Computational Fluid Dynamics (CFD) and Finite Element Method (FEM). Initially, we developed the CFD simulation to determine the aerodynamic forces acting on the wing. Next, we established the FEM simulation to analyze the deformation and stresses resulting from these aerodynamic loads. The final step involved coupling these two software tools. The CFD analysis provided us with approximately 954 Newtons of downforce at 100 km/h, which led to a maximum deformation of 2.2 mm, as determined by the FEM analysis. This maximum deformation occurred at the center of the trailing edge of Overwing 2. While we didn't have time to explore the potential impact of this deformation on the aerodynamic performance of the wing, further investigation into how it affects downforce could be valuable. Additionally, if the deformation significantly impacts downforce, we could look into improving the sandwich structure to enhance stiffness and reduce the deformation.

To conclude, we successfully achieved our goals by obtaining a favorable downforce value, designing a composite layup that is sufficiently stiff and stable, and validating our design through FSI simulation. This process confirmed that our design is safe and meets the required performance criteria and legality of Formula Student Rules.

Bibliography

[1] "Le Tunnel Hydrodynamique au Service de la Recherche Aérospatiale," by H. Werlé, 1974, ONERA [Werlé 1974].
[2] "Formula Student Rules 2024" [2024].
[3] "Introduction to Composite Materials" by Tri-Dung Ngo [2020].

A
Appendix

Ansys
2024 R1

Ansys Fluent Simulation Report

Analyst	Bilalmoh
Date	1/15/2025 07:47 PM

Table of Contents

System Information

Application	Fluent
Settings	3d, pressure-based, SST k-omega
Version	24.1.0-10184
Source Revision	5b3f9fb3c8
Build Time	Nov 22 2023 10:25:54 EST
CPU	12th Gen Intel(R) Core(TM) i5-12500
OS	Windows

Geometry and Mesh

Mesh Size

Cells	Faces	Nodes
25801869	51656002	4352251

Mesh Quality

Name	Type	Min Orthogonal Quality	Max Aspect Ratio
geom-1_solid	Tet Cell	1.3516868e-05	7970.7065

Orthogonal Quality

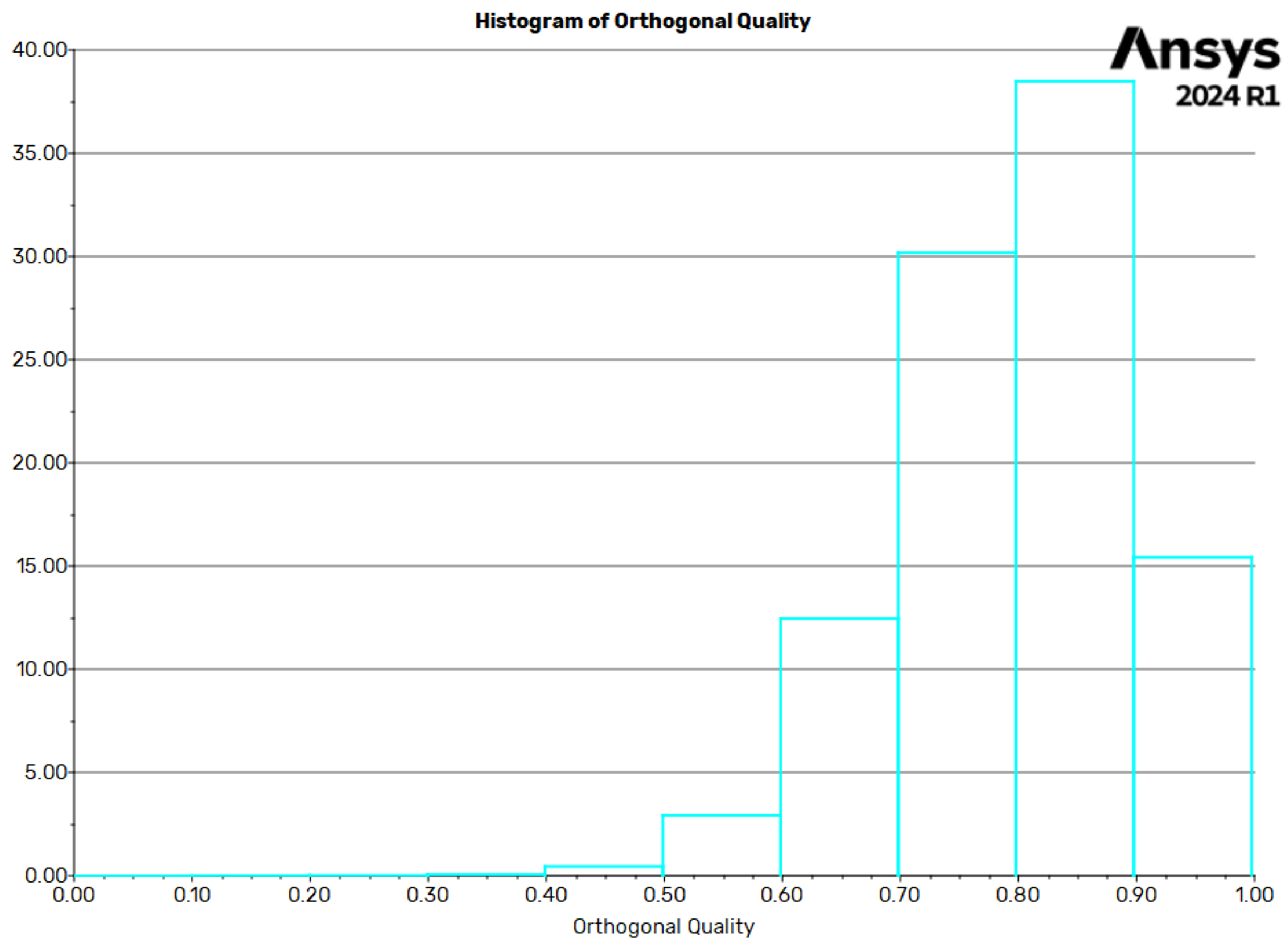

Simulation Setup

Physics

Models

Model	Settings
Space	3D
Time	Steady
Viscous	SST k-omega turbulence model

Material Properties

− Fluid	
− air	
Density	1.225 kg/m^3
Cp (Specific Heat)	1006.43 J/(kg K)
Thermal Conductivity	0.0242 W/(m K)
Viscosity	1.7894e-05 kg/(m s)
Molecular Weight	28.966 kg/kmol
− Solid	
− aluminum	
Density	2719 kg/m^3
Cp (Specific Heat)	871 J/(kg K)
Thermal Conductivity	202.4 W/(m K)

Cell Zone Conditions

− Fluid	
− geom-1_solid	
Material Name	air
Specify source terms?	no
Specify fixed values?	no
Frame Motion?	no
Laminar zone?	no
Porous zone?	no
3D Fan Zone?	no

Boundary Conditions

− Inlet	
− inlet	
Velocity Specification Method	Magnitude, Normal to Boundary
Reference Frame	Absolute

Velocity Magnitude [m/s]	27.7778
Supersonic/Initial Gauge Pressure [Pa]	0
Turbulent Specification Method	Intensity and Viscosity Ratio
Turbulent Intensity [%]	5
Turbulent Viscosity Ratio	10
− Outlet	
− outlet	
Backflow Reference Frame	Absolute
Gauge Pressure [Pa]	0
Pressure Profile Multiplier	1
Backflow Direction Specification Method	Normal to Boundary
Turbulent Specification Method	Intensity and Viscosity Ratio
Backflow Turbulent Intensity [%]	5
Backflow Turbulent Viscosity Ratio	10
Backflow Pressure Specification	Total Pressure
Build artificial walls to prevent reverse flow?	no
Radial Equilibrium Pressure Distribution	no
Average Pressure Specification?	no
Specify targeted mass flow rate	no
− Wall	
− wall	
Wall Motion	Stationary Wall
Shear Boundary Condition	No Slip
Wall Surface Roughness	rough bc standard
Wall Roughness Height [m]	0
Wall Roughness Constant	0.5
− wing	
Wall Motion	Stationary Wall
Shear Boundary Condition	No Slip
Wall Surface Roughness	rough bc standard
Wall Roughness Height [m]	0
Wall Roughness Constant	0.5

Reference Values

Area	1 m^2
Density	1.225 kg/m^3
Enthalpy	0 J/kg
Length	1 m
Pressure	0 Pa
Temperature	288.16 K
Velocity	1 m/s
Viscosity	1.7894e-05 kg/(m s)
Ratio of Specific Heats	1.4
Yplus for Heat Tran. Coef.	300

Solver Settings

− Equations	
Flow	True
Turbulence	True
− Numerics	
Absolute Velocity Formulation	True
− Pseudo Time Explicit Relaxation Factors	
Density	1
Body Forces	1
Turbulent Kinetic Energy	0.75
Specific Dissipation Rate	0.75
Turbulent Viscosity	1
Explicit Momentum	0.5
Explicit Pressure	0.5
− Pressure-Velocity Coupling	
Type	Coupled
Pseudo Time Method (Global Time Step)	True
− Discretization Scheme	
Pressure	Second Order
Momentum	Second Order Upwind
Turbulent Kinetic Energy	Second Order Upwind
Specific Dissipation Rate	Second Order Upwind
− Solution Limits	
Minimum Absolute Pressure [Pa]	1
Maximum Absolute Pressure [Pa]	5e+10
Minimum Static Temperature [K]	1
Maximum Static Temperature [K]	5000
Minimum Turb. Kinetic Energy [m^2/s^2]	1e-14
Minimum Spec. Dissipation Rate [s^-1]	1e-20
Maximum Turb. Viscosity Ratio	100000

Run Information

Number of Machines	1
Number of Cores	4
Case Read	75.453 seconds
Data Read	22.845 seconds
Virtual Current Memory	22.5041 GB
Virtual Peak Memory	23.996 GB
Memory Per M Cell	0.848062

Solution Status

Iterations: 147

	Value	Absolute Criteria	Convergence Status
continuity	0.000962962	0.001	Converged
x-velocity	1.72703e-07	0.001	Converged
y-velocity	1.06855e-07	0.001	Converged
z-velocity	1.235607e-07	0.001	Converged
k	0.0001808704	0.001	Converged
omega	1.127168e-05	0.001	Converged

Report Definitions

drag	412.0526	N
downforce	999.5239	N

Plots

Residuals

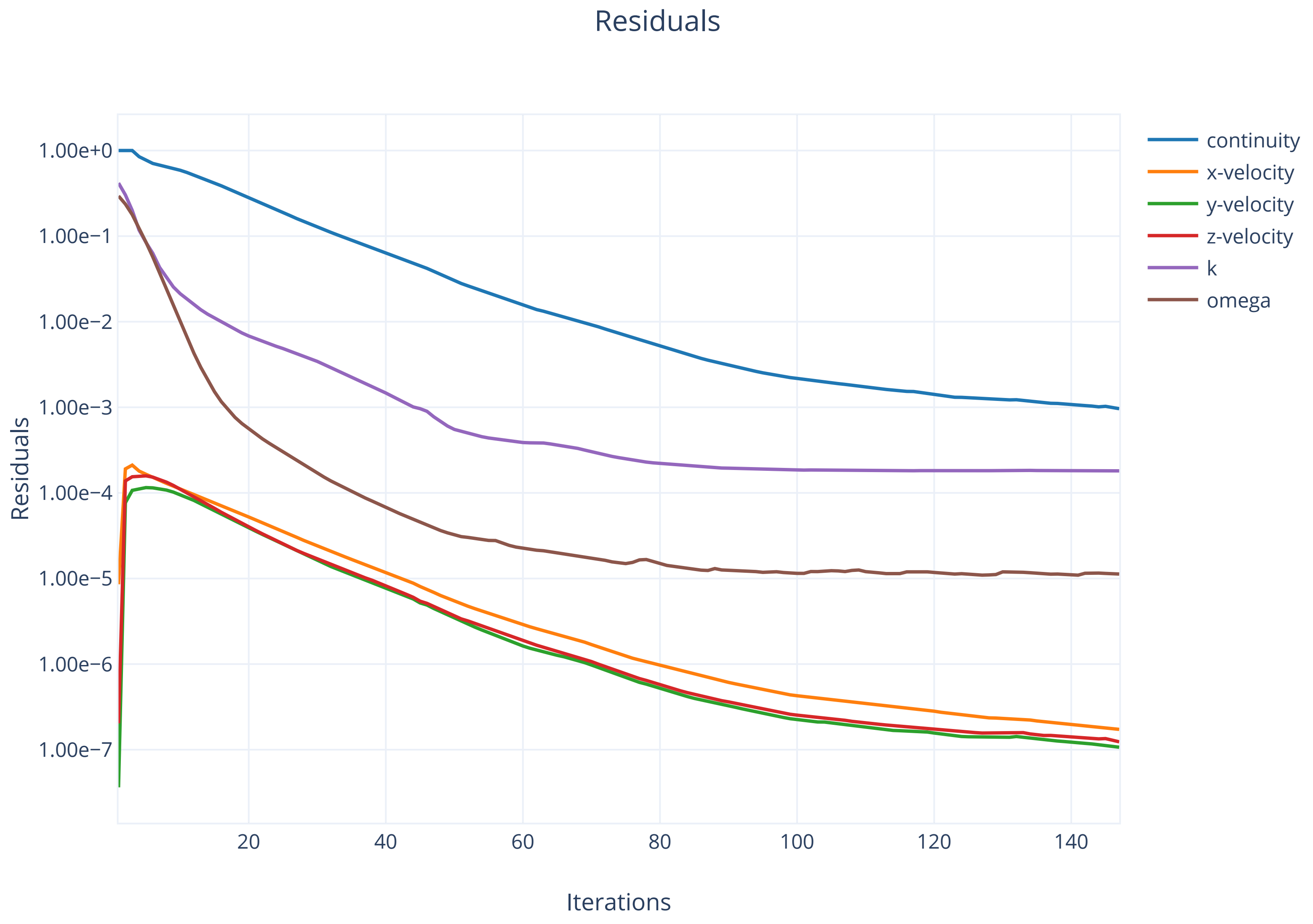

report-def-0-rplot

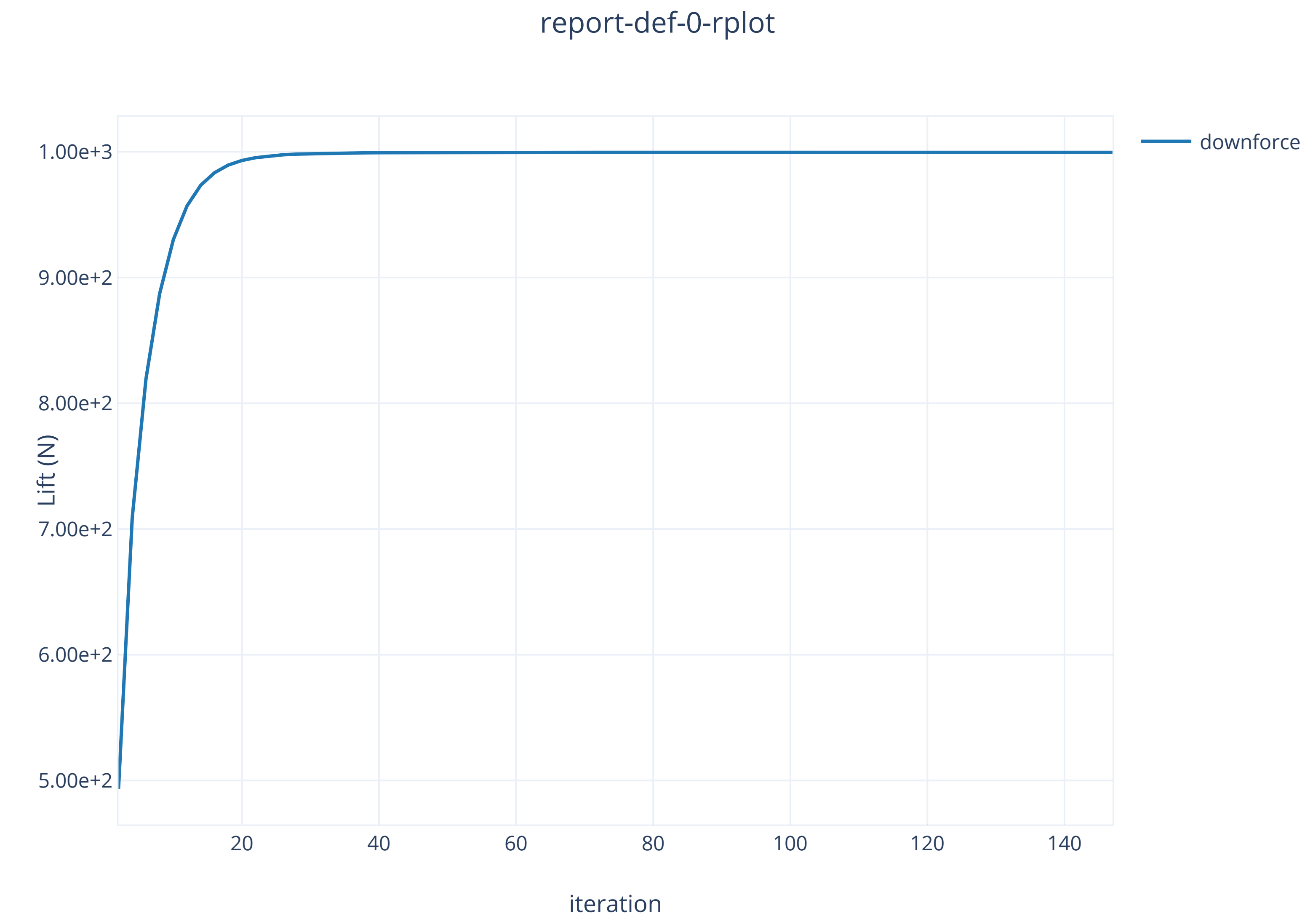

downforce-rplot

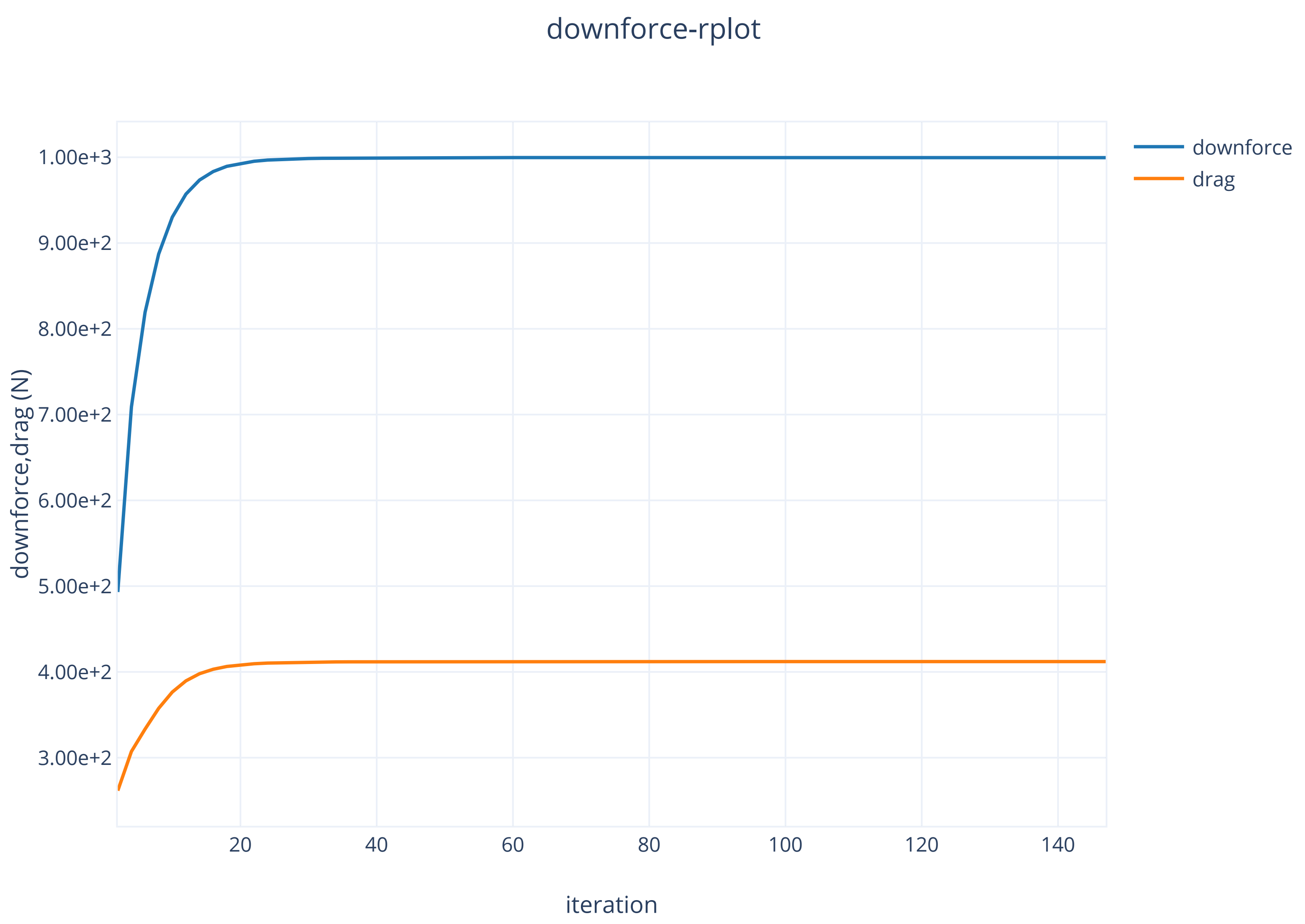

drag-rplot

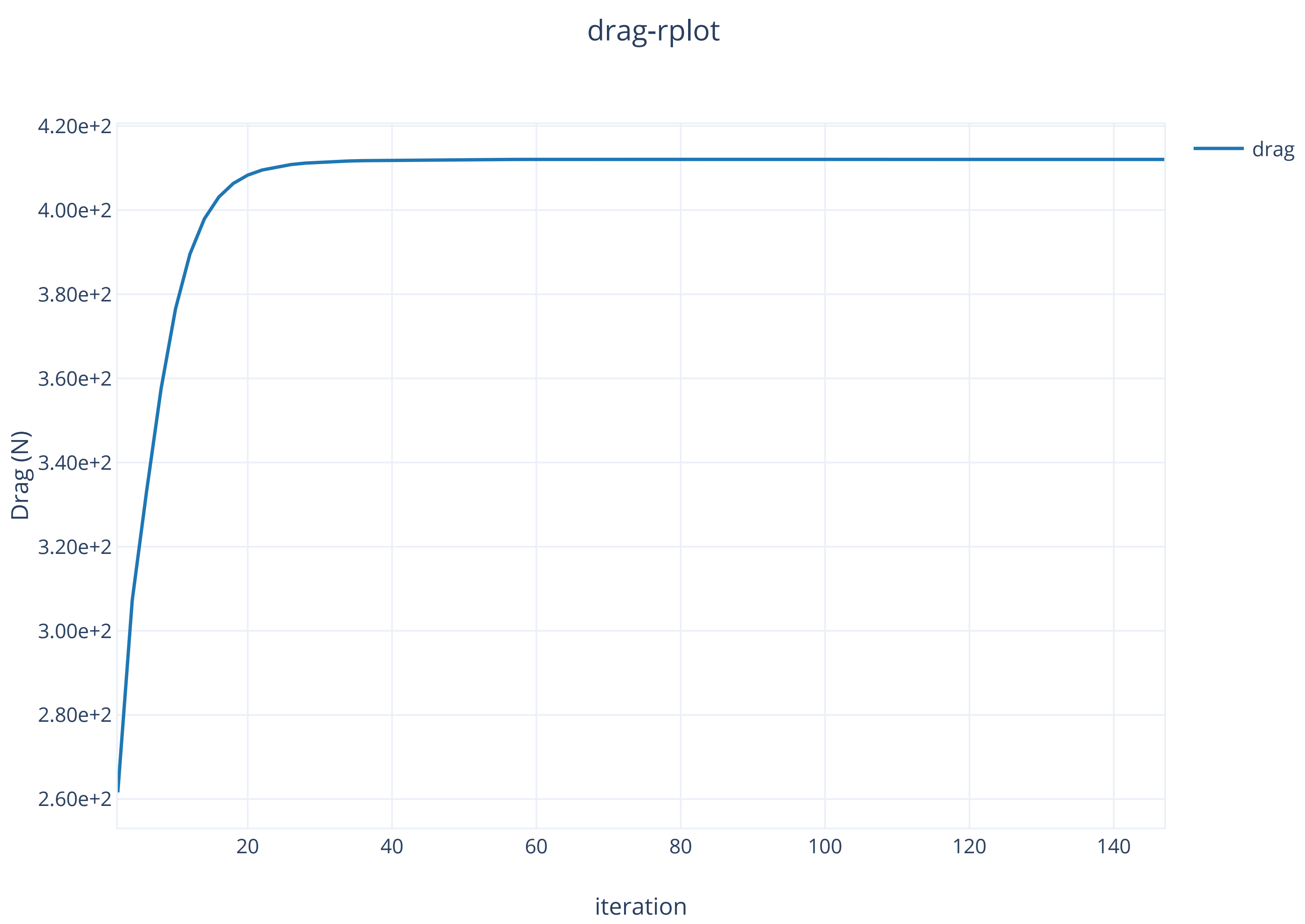

DEPARTMENT OF MECHANICAL ENGINEERING
CHALMERS UNIVERSITY OF TECHNOLOGY AND UNIVERSITY OF GOTHENBURG
Gothenburg, Sweden
www.chalmers.se

UNIVERSITY OF GOTHENBURG

CHALMERS
UNIVERSITY OF TECHNOLOGY